

**FEDSM2002-31049**

**TIME-DEPENDENT OPTIMAL PERTURBATIONS FOR THE ALGEBRAIC  
INSTABILITY IN THE NONLINEAR REGIME**

**Simone Zuccher\***

Dipartimento di Ingegneria Aerospaziale  
Politecnico di Milano  
Via La Masa 34  
20158 Milano, Italy  
Email: zuccher@asu.edu

**Paolo Luchini†**

Dipartimento di Ingegneria Meccanica  
Università di Salerno  
84084 Fisciano, Italy  
Email: luchini@unisa.it

**ABSTRACT**

The aim of the present study is to extend the linear unsteady optimal-perturbation analysis of (Luchini 2000) to the nonlinear regime. In order to account for the nonlinear interactions, a Fourier expansion is applied in the streamwise direction and in time and the solution is decomposed in Fourier modes along both  $z$  and  $t$ . The optimal unsteady spanwise-sinusoidal leading-edge excitation that provides the maximum energy growth for a given initial energy and frequency can thus be determined. Of interest will be that the optimal growth decreases with both.

**INTRODUCTION**

**Algebraic instability**

It is known that some instability mechanisms cannot be seen in the classical Orr–Sommerfeld formulation (eigenvalue-based linear stability theory). For instance, the stability analysis of Hagen-Poiseuille pipe flow reveals that all eigenfunctions are stable; nevertheless, if the Reynolds number is large enough, transition is experimentally observed.

An explanation was given by (Ellingsen & Palm 1975) and (Landahl 1980): they identified a new mechanism of disturbance amplification, according to which a longitudinal vortex superimposed to a two-dimensional boundary layer can lift up low-velocity fluid from the wall and push down high-velocity fluid

towards the wall. The disturbance accumulated over the streamwise length can be  $Re^{1/2}$  times greater than the original one since the structure of the boundary layer is elongated in the streamwise direction (with a typical length  $Re^{1/2}$  times greater than the boundary-layer thickness).

The combination of this basically inviscid amplification mechanism with the damping effect of viscosity leads to what is nowadays called *algebraic instability* or *transient growth*.

**Previous work**

Almost all previously published work in the field of algebraic instability is limited to a linearized analysis.

In the temporal stability framework, (Farrell 1988) computed the initial flow disturbance that produces the maximum gain (defined as the ratio between the perturbation kinetic energies at the final and initial time) in two dimensional plane channel flow. (Boberg & Brosa 1988) had already introduced a similar concept for flow in a pipe, but (Butler & Farrell 1992) gave the first quantitative calculation of three-dimensional optimal perturbations with respect to temporal growth, not only for plane Couette and Poiseuille flow, but also for a parallel approximation of the Blasius boundary layer. (Corbett & Bottaro 2000) found the temporal-growth optimal perturbations for parallel boundary layers subject to streamwise pressure gradient considering Falkner–Skan base flow profiles and (Corbett & Bottaro 2001) studied the temporal growth in swept boundary layers described by Falkner–Skan–Cooke similarity solution.

---

\*Present address: Mechanical and Aerospace Engineering, Arizona State University, Tempe AZ 85287

†Address all correspondence to this author.

The problem of spatial stability for a Blasius boundary layer was tackled by Luchini (1997, 2000) and by Andersson, Berggren & Henningson (1998, 1999). An adjoint-based optimization technique was used in order to determine the optimal perturbation profile at  $x = 0$  and the gain, defined as the energy disturbance at the output divided by the energy disturbance at the leading edge. The optimal spanwise wavenumber for a steady linear perturbation was found to be  $\beta = 0.45$ . Like previous authors, they observed that the optimal initial disturbance is composed of stationary streamwise vortices whereas the induced velocity field is dominated by streamwise streaks.

Luchini (2000) also considered the possibility of unsteady disturbances, computing the gain as a function of frequency for the steady optimal wavenumber ( $\beta = 0.45$ ). Results showed that the maximum gain corresponds to steady initial perturbations ( $\omega = 0$ ), and that for increasing frequency the gain monotonically decreases.

Andersson, Brandt, Bottaro & Henningson (2001) investigated via direct numerical simulation the subsequent nonlinear evolution of the optimal perturbations provided by the linear approach (those computed by (Luchini 2000) and (Andersson *et al.* 1999)), focusing upon the secondary temporal instability of the produced streaks. They did not actually optimize any perturbations in the nonlinear case.

Steady nonlinear optimal perturbations were first computed by Zuccher, Luchini & Bottaro (2002). They solved the nonlinear steady boundary layer equations by decomposing the velocity field in a Fourier series along the spanwise direction, so that full generality was allowed in considering their interaction and the nonlinear effects induced by them. Their work showed that the optimal wavenumber decreases when the initial energy increases.

The main goal of this work is to extend the nonlinear study performed by (Zuccher *et al.* 2002) to the unsteady case of (Luchini 2000), so as to compute the optimal unsteady leading-edge excitation that provides the maximum gain for a given initial energy.

## PROBLEM FORMULATION

(Zuccher *et al.* 2002), in order to find optimal perturbations for the nonlinear algebraic instability of an incompressible boundary layer over a flat plate, considered the general steady three-dimensional incompressible boundary-layer equations, in conservative form, and written in boundary-layer variables typical of three-dimensionalities originating inside the boundary layer itself. Here we solve the corresponding unsteady equations:

$$\begin{aligned} u_x + v_y + w_z &= 0 \\ u_t + (uu)_x + (uv)_y + (uw)_z - u_{yy} - u_{zz} &= 0 \\ v_t + (uv)_x + (vv)_y + (vw)_z + p_y - v_{yy} - v_{zz} &= 0 \\ w_t + (uw)_x + (vw)_y + (ww)_z + p_z - w_{yy} - w_{zz} &= 0 \end{aligned} \quad (1)$$

where the  $u$  velocity component is made dimensionless with respect to the outer velocity  $U_\infty$  and the  $v$  and  $w$  (respectively wall-normal and spanwise) components are made dimensionless with respect to  $Re^{-1/2}U_\infty$ .  $Re$  is the Reynolds number defined as  $Re = U_\infty L/\nu$ . The streamwise coordinate  $x$  is normalized with a reference length  $L$ , the wall-normal coordinate  $y$  and the spanwise coordinate  $z$  are made dimensionless with  $\delta = Re^{-1/2}L = (\nu L/U_\infty)^{1/2}$  and time is normalized with respect to  $L/U_\infty$ .  $p$ , the second-order term in the inner expansion of pressure, is made dimensionless with respect to  $Re^{-1}\rho U_\infty^2$ . System (1) requires six boundary conditions, three at the wall, where  $y = 0$ , and three for  $y \rightarrow \infty$

$$\begin{aligned} u &= 0 \text{ at } y = 0 & u &= 1 \text{ for } y \rightarrow \infty \\ v &= 0 \text{ at } y = 0 & w &= 0 \text{ for } y \rightarrow \infty \\ w &= 0 \text{ at } y = 0 & p &= 0 \text{ for } y \rightarrow \infty \end{aligned} \quad (2)$$

and two initial conditions ( $w$  is uniquely determined once  $u$  and  $v$  have been assigned, see (Zuccher *et al.* 2002)). When the streamwise component upstream of the leading edge, is uniformly  $u = 1$ , the constraint relating the initial conditions for  $v$  and  $w$  simply reduces to the continuity equation so that the initial conditions read:

$$\begin{aligned} u(0, y, z, t) &= 1 \\ v(0, y, z, t) &= v_0(y, z, t) \end{aligned} \quad (3)$$

System (1) with initial conditions (3) and boundary conditions (2) represents the direct or forward problem to be solved.

In order to perform an optimization, an objective function needs to be specified. For this purpose the perturbation kinetic energy is generally taken as a measure of the perturbation level, even if this is not necessarily the only physical quantity signalling transition. Accordingly, our objective function will be the gain at the outlet  $\mathcal{J} = G_{\text{out}}$ , defined as the ratio between the energy at the outlet and the initial energy. In the boundary-layer limit of infinite Reynolds number,  $G_{\text{out}}$  reads

$$G_{\text{out}} = \frac{E_{\text{out}}}{E_{\text{in}}} = Re \frac{\left[ \int_{-T}^T \int_{-Z}^Z \int_0^\infty [|\bar{u}|^2] dy dz dt \right]_{x=1}}{\left[ \int_{-T}^T \int_{-Z}^Z \int_0^\infty (|\bar{v}|^2 + |\bar{w}|^2) dy dz dt \right]_{x=0}} \quad (4)$$

## Constrained optimization

We want to find the initial condition  $\bar{v}_0(y, z, t)$  for the wall-normal velocity component at  $x = 0$  which makes the objective function  $G_{\text{out}}$  an extremum for a given initial energy  $E_0$ . For this reason, we impose the constraint  $E_{\text{in}} = E_0$  where the initial

energy  $E_{\text{in}}$  is

$$E_{\text{in}} = \left[ \int_{-T}^T \int_{-Z}^Z \int_0^\infty [|\bar{v}|^2 + |\bar{w}|^2] dy dz dt \right]_{x=0} = E_0 \quad (5)$$

but since  $\bar{w}_0$  is related to  $\bar{v}_0$ , the initial perturbation energy can be seen as depending on  $\bar{v}_0$  only:  $E_{\text{in}}(\bar{v}_0) = E_0$ .

The technique of Lagrange multipliers is used to solve the constrained optimization problem. For this purpose we introduce a suitable functional  $\mathcal{L}$ , where the continuity and momentum equations are multiplied by  $a(x, y, z, t)$ ,  $b(x, y, z, t)$ ,  $c(x, y, z, t)$ ,  $d(x, y, z, t)$  and integrated over all space and time and the initial-energy constraint is multiplied by  $\lambda_0$ . Maximizing  $\mathcal{L}$  implies that its variation  $\delta\mathcal{L}$  must be vanishing for unconstrained variations in all the parameters which it depends upon. As in (Zuccher *et al.* 2002), it can be easily seen that the Fréchet derivatives of the functional  $\mathcal{L}$  with respect to the Lagrange multipliers  $a, b, c, d, \lambda_0$  reproduce the original constraints, respectively system (1) and the energy constraint (5), while the derivatives of the functional with respect to the direct variables  $u, v, w, p$ , after integration by parts, produce the set of adjoint equations:

$$\begin{aligned} c_y + d_z &= 0 \\ -b_t + a_x^* - 2u_x b + b_y v + b_z w + c_z v + d_x v + d_x w + b_{yy} + b_{zz} &= 0 \\ -b_t + a_y^* - 2b u_y - b_y u + c_x u + 2c_y v + d_y w + c_z w + c_{yy} + c_{zz} &= 0 \\ -b_t + a_z^* - 2b u_z - b_z u + c_z v + d_y v + d_x u + 2d_z w + d_{yy} + d_{zz} &= 0 \end{aligned} \quad (6)$$

where  $a^* = a + 2bu$ . This system is parabolic, just as the direct system, but the marching direction of stable evolution is backwards from the outlet  $x = 1$  to  $x = 0$ , so that initial conditions are required at  $x = 1$ . These are provided by the set of conditions arising from the boundary terms (at  $x = 0$ ,  $x = 1$ ,  $y = 0$  and for  $y \rightarrow \infty$ ) left over by the integration by parts. At the same time, an initial condition at  $x = 0$  for the direct problem is obtained from the derivative with respect to  $\bar{v}_0$ : it couples the direct to the adjoint solution in the course of the constrained optimization. The boundary conditions for system (6) are:

$$\begin{aligned} b &= 0 \text{ at } y = 0 & c &= 0 \text{ for } y \rightarrow \infty \\ a^* - 2bu + c_y &= 0 \text{ at } y = 0 & a^* - ub + c_y &= 0 \text{ for } y \rightarrow \infty \\ d &= 0 \text{ at } y = 0 & d &= 0 \text{ for } y \rightarrow \infty \end{aligned} \quad (7)$$

and the initial conditions at  $x = 1$  read

$$\begin{aligned} c &= 0 & \text{at } x &= 1 \\ d &= 0 & \text{at } x &= 1 \\ a^* + \frac{\delta G_{\text{out}}}{\delta u} &= 0 & \text{at } x &= 1 \end{aligned} \quad (8)$$

The coupling condition at  $x = 0$ , which relates the direct and

adjoint problem, reduces to

$$c + \lambda_0 \frac{\delta E_{\text{in}}}{\delta \bar{v}} = 0 \text{ at } x = 0 \quad (9)$$

We solve this system by an iteration technique based on the fact that, when seen separately, the direct equations are parabolic in the forward and the adjoint equations in the backward direction. This iteration involves alternating the solution of the direct and adjoint equations, and repeating until a converged solution is attained. At this point  $\delta\mathcal{L} = 0$  will have been achieved. A similar procedure was also used by (Luchini 2000) for the corresponding linear problem. In the nonlinear case, however, convergence can only be achieved through a successive-bisection search, where the value of the objective function is checked for monotonic increase after every step. The reader is referred to (Zuccher *et al.* 2002) for further details.

## IMPLEMENTATION AND NUMERICAL SOLUTION

### Direct and adjoint solutions

For the purpose of numerical discretization, the solution of the direct problem is expanded in a Fourier series along the spanwise direction  $z$  and in time  $t$ . If

$$f(x, y, z, t) = \sum_{n=-N}^{+N} \sum_{m=-M}^{+M} F_{nm}(x, y) e^{in\beta z - im\omega t} \quad (10)$$

represents the general quantity  $u, v, w, p$ , the function  $F_{nm}(x, y)$  is the complex amplitude of the  $n^{\text{th}}$  mode in  $z$  and the  $m^{\text{th}}$  mode in  $t$  and only depends on  $x$  and  $y$ .

Under the previous expansion, the nonlinear terms in equations (1) produce a double summation containing a convolution. For example, denoting by  $f(x, y, z, t)$  and  $g(x, y, z, t)$  two generic variables among  $(u, v, w)$ , one has:

$$f(x, y, z, t)g(x, y, z, t) = \sum_{n=-N}^{+N} \sum_{m=-M}^{+M} e^{in\beta z - im\omega t} C_{nm}^{FG}(x, y) \quad (11)$$

where

$$C_{nm}^{FG}(x, y) = \sum_{k=a}^b \sum_{h=c}^d F_{kh}(x, y) G_{n-k, m-h}(x, y) \quad (12)$$

and  $a = \max(-N, n + N)$ ;  $b = \min(N, n - N)$ ;  $c = \max(-M, m + M)$ ;  $d = \min(M, m - M)$ . Introducing ex-

pressions (10) into equations (1) yields:

$$\begin{aligned}
(U_{nm})_x + (V_{nm})_y + in\beta W_{nm} &= 0 \\
-im\omega U_{nm} + (C_{nm}^{UU})_x + (C_{nm}^{UV})_y + \\
in\beta C_{nm}^{UW} - (U_{nm})_{yy} + n^2\beta^2 U_{nm} &= 0 \\
-im\omega V_{nm} + (C_{nm}^{VV})_x + (C_{nm}^{VW})_y + \\
in\beta C_{nm}^{VW} - (V_{nm})_y + n^2\beta^2 V_{nm} + (P_{nm})_y &= 0 \\
-im\omega W_{nm} + (C_{nm}^{UW})_x + (C_{nm}^{VW})_y + \\
in\beta C_{nm}^{WW} - (W_{nm})_{yy} + n^2\beta^2 W_{nm} + in\beta P_{nm} &= 0
\end{aligned} \tag{13}$$

For this parabolic system in  $x$  and  $y$  we choose a second-order implicit backward-Euler finite-difference discretization. In addition, a non uniform grid is used in either direction, which becomes finer near the leading edge in  $x$  and near the wall in  $y$ .

After discretization, system (1) becomes a system of nonlinear algebraic equations, an iterative solution of which is required. The nonlinear coefficients  $C_{nm}^{FG}(x,y)$  couple every mode of each variable ( $u, v, w, p$ ) to every other one and therefore a complete Newton linearization would involve a relatively large linear system, which needs a large amount of memory and a large computational time in order to be solved. For this reason, according to the procedure already tested in (Zuccher *et al.* 2002), we adopt an incomplete linearization and decouple the different modes ( $n,m$ ) so that a separate narrow-banded system must be solved for each mode. In any case, at convergence the same exact solution is obtained as from the complete Newton iteration.

The adjoint problem, following the same approach as (Zuccher *et al.* 2002), (Cathalifaud & Luchini 2000) and (Luchini & Bottaro 1998), is solved by taking the adjoint of the discrete direct equations, thus gaining the possibility of a perfect test that can be obtained by comparing the results of the direct and adjoint calculation for any step size and not only in the limit of step size tending to zero. Since an optimization using the discrete adjoint produces the exact optimum of the discretized problem, the correct result can be guaranteed if only the discrete direct problem is a consistent approximation of the continuous direct problem, without any additional need to verify the consistency of the adjoint problem.

The adjoint problem is solved by a similar incomplete Newton iteration (which in this case amounts to an iterative solution of a linear system of algebraic equations), while marching in the backward direction from  $x = 1$  to  $x = 0$ .

## RESULTS

In the following we shall assume a sinusoidal dependence of the initial perturbation  $v_0$  on the spanwise coordinate  $z$  and on time  $t$ , so that only mode (0,0), which represents the base flow,

and modes  $(\pm 1, \pm 1)$ , which represent a sinusoidal perturbation in  $z$  and/or  $t$ , are present at  $x = 0$ . Two cases will be considered: a travelling wave, where only mode (1,1) and its complex conjugate are present, and a standing wave, where all four modes  $(\pm 1, \pm 1)$  are simultaneously present.

In figure 1 the gain is reported as a function of wavenumber  $\beta$  for different values of the initial energy  $E_0$  and for the steady case ( $\omega = 0$ ). The linear result (solid line) corresponds to figure 1 of (Luchini 2000). As found by (Zuccher *et al.* 2002), when the initial energy increases the optimal wavenumber, defined as the wavenumber for which the gain is maximum, decreases. There is a difference between this figure and the corresponding figure of (Zuccher *et al.* 2002) in that the objective function here is the final energy  $E_{out}$ , whereas in the former paper it was the average energy over the complete length of the boundary layer. The overall qualitative behaviour is unchanged, but the optimal wavenumber changes by roughly 20% depending on the objective function.

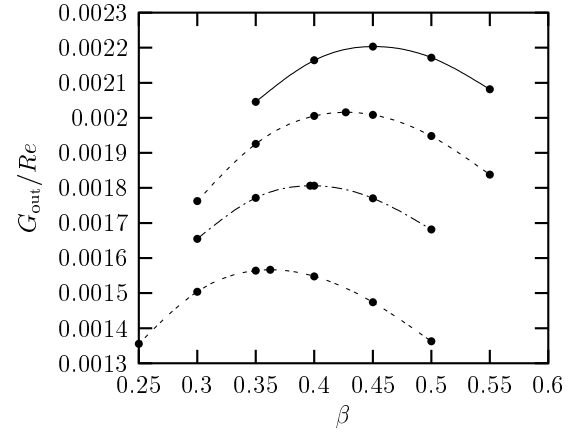


Figure 1. GAIN AS A FUNCTION OF  $\beta$  FOR DIFFERENT VALUES OF THE INITIAL ENERGY  $E_0$ , STEADY CASE ( $\omega = 0$ ).

Linear: —;  $E_0 = 200$ : - - - -;  $E_0 = 500$ : - · - · - ·;  $E_0 = 1000$ : · · · · ·.

The effect of nonlinearities at non zero frequency is illustrated in figure 2, which reports the dependence of the gain on the initial energy for various frequencies and a wavenumber  $\beta = 0.45$ , corresponding to the optimal wavenumber in the linear and steady case. It can be observed that also in the nonlinear regime the maximum amplification occurs for  $\omega = 0$ , and the decrease of gain with both frequency and initial energy is monotonic.

Results reported in figure 2 have been obtained using  $N = 3$  and  $M = 3$  modes. In order to check the dependence on the number of modes, further tests have been performed using  $N = 4$ ,  $M = 3$  for  $E_0 = 200$  and  $E_0 = 500$  finding no appreciable change

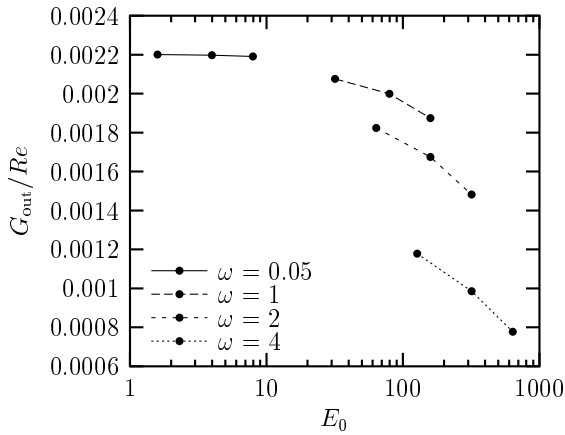


Figure 2. GAIN AS A FUNCTION OF  $E_0$  FOR DIFFERENT VALUES OF THE FREQUENCY  $\omega$ , AT  $\beta = 0.45$ .

of gain in the first case, and a relative change of  $10^{-5}$  in the second. Since the computational cost increases rapidly with the number of modes, further tests may require significant changes in the numerical method.

In figure 3 the  $v$  component of the optimal perturbation at  $x = 0$  is reported for the steady case and different values of the initial energy, at a fixed wavenumber  $\beta = 0.45$ . The behavior is

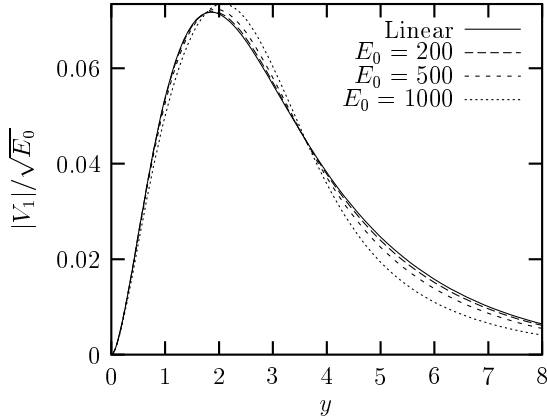


Figure 3.  $V$  COMPONENT OF THE OPTIMAL PERTURBATION FOR  $\omega = 0$  AND DIFFERENT VALUES OF THE INITIAL ENERGY  $E_0$ , AT FIXED OPTIMAL WAVENUMBER  $\beta = 0.45$ .

quite regular and the maximum moves away from the wall as  $E_0$  increases.

In figure 4 the  $w$  component of the optimal perturbation at  $x = 0$  is reported for the steady case and different values of the initial energy, at fixed wavenumber  $\beta = 0.45$ . Since the initial  $w$

is proportional to  $v_y$ , its profile goes to zero where the  $v$  component reaches its maximum.

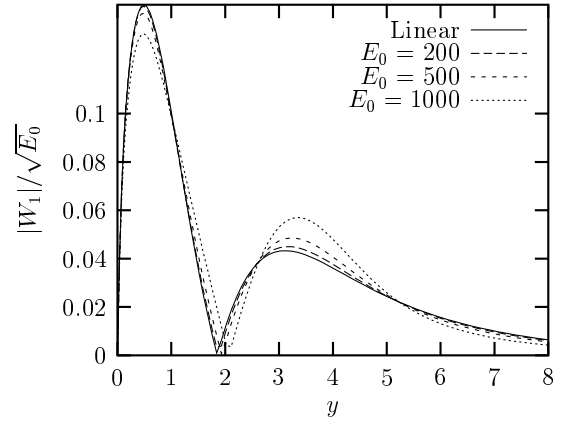


Figure 4.  $W$  COMPONENT OF THE OPTIMAL PERTURBATION FOR  $\omega = 0$  AND DIFFERENT VALUES OF THE INITIAL ENERGY  $E_0$ , AT FIXED OPTIMAL WAVENUMBER  $\beta = 0.45$ .

In figure 5 the energy growth is shown for the steady case and different values of the initial energy, at fixed wavenumber  $\beta = 0.45$ . The curve decreases and tends to become flatter for

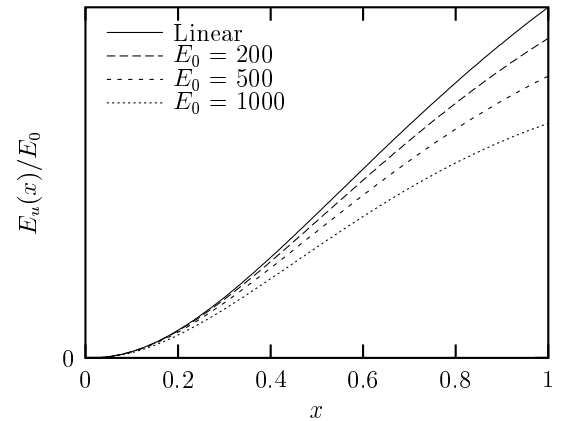


Figure 5. ENERGY AS A FUNCTION OF THE STREAMWISE COORDINATE FOR  $\omega = 0$  AND DIFFERENT VALUES OF THE INITIAL ENERGY  $E_0$ , AT FIXED OPTIMAL WAVENUMBER  $\beta = 0.45$ .

increasing initial energy, as observed by (Zuccher *et al.* 2002) when maximizing the mean energy.

In figure 6 the  $v$  component of the optimal perturbation is shown for the linear case and different values of  $\omega$ , at fixed

wavenumber  $\beta = 0.45$ . The position of the maximum moves

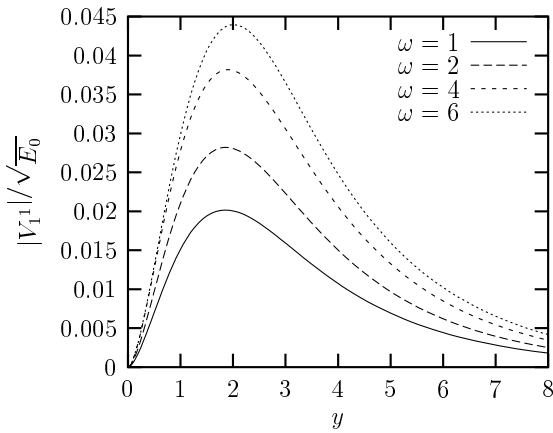


Figure 6. V COMPONENT OF THE OPTIMAL PERTURBATION FOR THE LINEAR CASE AND DIFFERENT VALUES OF  $\omega$ , AT FIXED OPTIMAL WAVENUMBER  $\beta = 0.45$ .

away from the wall and its value increases for increasing  $\omega$ , but the behavior seems otherwise quite regular.

On the other hand, figure 7 shows a visible difference between the steady and unsteady optimal perturbations. The absolute value of the  $w$  component of the optimal perturbation at  $x = 0$  no longer passes through zero because  $v$  and  $w$  are generic complex functions of  $y$ .

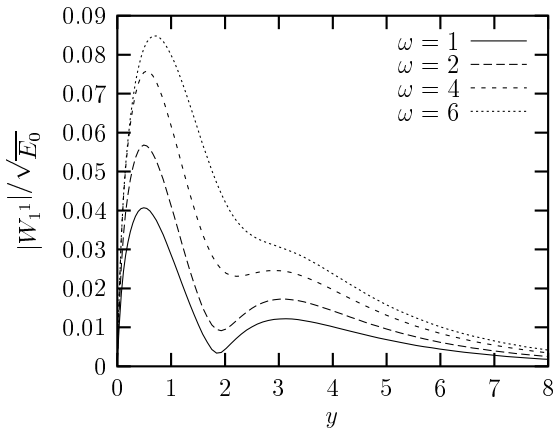


Figure 7. V COMPONENT OF THE OPTIMAL PERTURBATION FOR THE LINEAR CASE AND DIFFERENT VALUES OF  $\omega$ , AT FIXED OPTIMAL WAVENUMBER  $\beta = 0.45$ .

The energy growth for the linear case and different values of

$\omega$ , at  $\beta = 0.45$ , is reported in figure 8. At high frequency a plateau

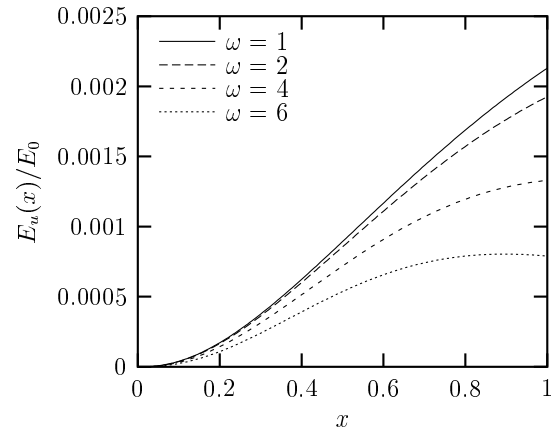


Figure 8. ENERGY AS A FUNCTION OF THE STREAMWISE COORDINATE FOR THE LINEAR CASE AND DIFFERENT VALUES OF  $\omega$ , AT FIXED OPTIMAL WAVENUMBER  $\beta = 0.45$ .

is observed, which resembles the plateau observed by (Zuccher *et al.* 2002) in the case of high wavenumber for  $\omega = 0$ .

## REFERENCES

- ANDERSSON, P., BERGGREN, M. & HENNINGSON, D.S. 1998 Optimal disturbances in boundary layers. *AFOSR Workshop on Optimal Design & Control*, Arlington VA, USA, 30 Sept.-3 Oct. 1997 (J.T. Borggaard, J. Burns, E. Cliff & S. Schreck eds.) Birkhauser, Boston.
- ANDERSSON, P., BERGGREN, M., & HENNINGSON, D. S. 1999 Optimal disturbances & bypass transition in boundary layers. *Phys. Fluids* **11**, 134–150.
- ANDERSSON, P., BRANDT, L., BOTTARO, A., & HENNINGSON, D. S. 2001 On the breakdown of boundary layer streaks. *J. Fluid Mech.* **428**, 29–60.
- BOBERG, B. & BROSA, G. 1988 Onset of turbulence in a pipe. *Z. Naturforschung* **43a**, 697–726.
- BUTLER, K. M., & FARRELL, B. 1992 Three-dimensional optimal perturbations in viscous shear flow. *Phys. Fluids* **A4**, 1637–1650.
- CATHALIFAUD, P., & LUCHINI, P. 2000 Algebraic growth in boundary layers: optimal control by blowing & suction at the wall. *Eur. J. Mech. B – Fluids* **19**, 469–490.
- CORBETT, P., & BOTTARO, A. 2000 Optimal perturbations for boundary layers subject to stream-wise pressure gradient. *Phys. Fluids* **12**, 120–130.
- CORBETT, P., & BOTTARO, A. 2001 Optimal linear growth in swept boundary layers. *J. Fluid Mech* **435**, 1–23.

ELLINGSEN, T. & PALM E. 1975 Stability of linear flow. *Phys. Fluids* **18**, 487–488.

FARRELL, B. 1988 Optimal excitation of perturbations in viscous shear flow. *Phys. Fluids* **31**, 2093–2102.

LANDAHL, M. T. 1980 A note on an algebraic instability of inviscid parallel shear flow. *J. Fluid Mech.* **98**, 243–251.

LUCHINI, P. 1996 Reynolds-number-independent instability of the boundary layer over a flat surface. *J. Fluid Mech.* **327**, 101–115.

LUCHINI, P. 1997 Effects on a flat-plate boundary layer of free-stream longitudinal vortices: optimal perturbations. *EUROMECH 3rd European Fluid Mechanics Conference*, Göttingen 15-18 Sept. 1997, DLR, Göttingen, p. 219.

LUCHINI, P., & BOTTARO, A. 1998 Görtler vortices: a backward-in-time approach to the receptivity problem. *J. Fluid Mech.* **363**, 1–23.

LUCHINI, P. 2000 Reynolds-number-independent instability of the boundary layer over a flat surface: optimal perturbations. *J. Fluid Mech.* **404**, 289–309.

ZUCCHER, S., LUCHINI, P., & BOTTARO, A. 2002 Optimal perturbation of the three-dimensional algebraically growing instability for a Blasius boundary layer in the nonlinear regime. *J. Fluid Mech.* Submitted.